Towards a sustainable synthesis of aromatic isocyanates : by the palladium diphosphane catalyzed reduction of nitrobenzene; a first step

Mooibroek, T.J.

Chapter 2

Complex formation and structure

Abstract: In this chapter the synthetic pathways towards Pd^{II} complexes of functionalized bidentate diphenylphosphane ligands of the type [Pd(ligand)(anion)$_2$] and [Pd(ligand)$_2$](anion)$_2$ is described. Eighteen different ligands have been used in combination with strongly (acetate, OAc^-) or weakly (tosylate, OTs^-) coordinating anions. Of some representative complexes the solid state structure was determined with X-ray crystallography. It is shown that the solid state structures are fully retained in solution. The formation of [Pd(ligand)(anion)$_2$]-type complexes was studied in detail using ^{1}H- and ^{31}P-NMR spectroscopy.
Depending on the ligand structure the complex is formed instantaneously, *via* a polynuclear intermediate or is not formed at all. Complex formation is demonstrated to depend on the length and rigidity of the ligand backbone, and on the steric bulk at the ortho position of the phenyl rings on phosphorus. It was also found that the coordinating ability of the anions can alter the structure of the kinetic and/or the thermodynamic product.

2.1 Introduction

For some decades, Pd^{II}-diphosphane catalytic systems have enjoyed much attention, both from academia and industry. Especially the copolymerization of CO and ethene has been widely studied[1, 2] and applied (Carilon®(Shell) and Ketonex® (BP)) using such catalytic systems. A reaction, in which these palladium catalysts are relatively poorly studied, is the carbonylation of nitroaromatic molecules to aromatic isocyanates.[3-8] For this reaction most endeavours involve catalysts of the type $[Pd^{II}(1,10\text{-phenanthroline})_2](anion)_2$,[4-8, 10-19] and only few involve catalysts of the type P_2Pd^{II}.[4, 17, 20, 21] Since there is no fundamental reason why N_2Pd^{II} complexes should perform better than P_2Pd^{II} complexes, in the present thesis the focus lies on studying these palladium-phosphane complexes in the carbonylation of nitrobenzene. In many catalytic studies the catalyst is often formed *in situ* by mixing a palladium^{II} salt with a diphosphane ligand in methanol, assuming that the desired [Pd(diphosphane)$(anion)_2$]-type complexes are actually formed. However, complex formation is not always a trivial process. For example, for the copolymerization of CO and ethene it has been reported that the catalytic performance of *in situ* formed catalysts may be inferior to that of the preformed catalysts.[23]

It has also been reported that when $[Pd(OAc)_2]$ and an equimolar amount of dppe (1,2-bis(diphenylphosphanyl)ethane) are dissolved in CD_3OD, initially the catalytically inactive complex $[Pd(dppe)_2](OAc)_2$ is formed; only after standing for about 24 hours, the catalytically active species $[Pd(dppe)(OAc)_2]$ is obtained.[24]

To the best of my knowledge, there is no simple way to predict the exact kinetic pathway *via* which a certain ligand will or will not form the desired [Pd(diphosphane)$(anion)_2$]-type complex. Therefore, the present chapter describes a study to determine the influence of the bridging groups and substituents in chelating diphosphane ligands (see Table 2.1) on the kinetics and the result of complex formation. Furthermore, the role of the anion in the complex formation process was investigated by using acetate (strongly coordinating) and tosylate (weakly coordinating) anions. Prior to this, however, the synthesis of this type of complexes is reported, followed by their structural characteristics in the solid phase and in solution.

Table 2.1. Schematic representation of the ligands used in this study. The inset figures show the general structures.

Code	X	R	Schematic drawing
L2	H		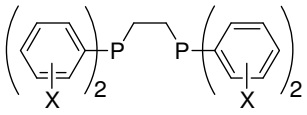
oMeO-L2	*o*-MeO		
oEtO-L2	*o*-EtO		
L3	H	H	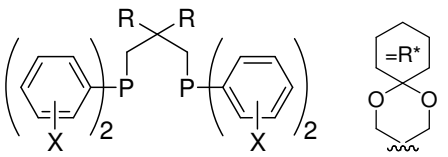
L3X	H	CH_3	
oMe-L3	*o*-Me	H	
oMeO-L3	*o*-MeO	H	
oEtO-L3	*o*-EtO	H	
pMeO-L3	*p*-MeO	H	
oMeO-L3X	*o*-MeO	CH_3	
oMeO-L3X[2]	*o*-MeO	CH_2CH_3	
oEtO-L3X[2]	*o*-EtO	CH_2CH_3	
oMeO-L3X[R]	*o*-MeO	R*	
L4	H	H	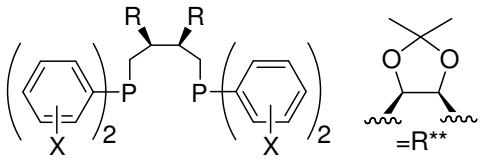
oMeO-L4	*o*-MeO	H	
oEtO-L4	*o*-EtO	H	
pMeO-L4	*p*-MeO	H	
L4X	H	R**	
oMeO-L4X	*o*-MeO	R**	

2.2 Results and discussion

2.2.1. Complex synthesis

Starting from crystalline $[Pd_3(OAc)_6]$,[25] four solvents were employed in the complex synthesis. In order of increasing polarity these are: $CHCl_3$, CH_2Cl_2, $(CH_3)_2CO$ and CH_3OH. The methods by which the desired complexes can successfully be obtained are summarized schematically in Figure 2.1. However, some difficulties were encountered in the synthesis and isolation of these complexes. Dry and degassed solvents must be used as too much water generally hampered the isolation due to the formation of an oil and partial oxidation of the ligand. Furthermore, the flasks were wrapped in foil; the absence of light in most cases prevented plating of Pd^0. The choice of the solvent appeared to be most important. $CHCl_3$ must be avoided since severe plating was usually observed when working with this solvent. CH_2Cl_2 and $(CH_3)_2CO$ were best suited for the synthesis of the monochelate [Pd(ligand)(anion)$_2$]–type complexes. Methanol is the only solvent in which the bischelate [Pd(ligand)$_2$](OAc)$_2$–type complexes can

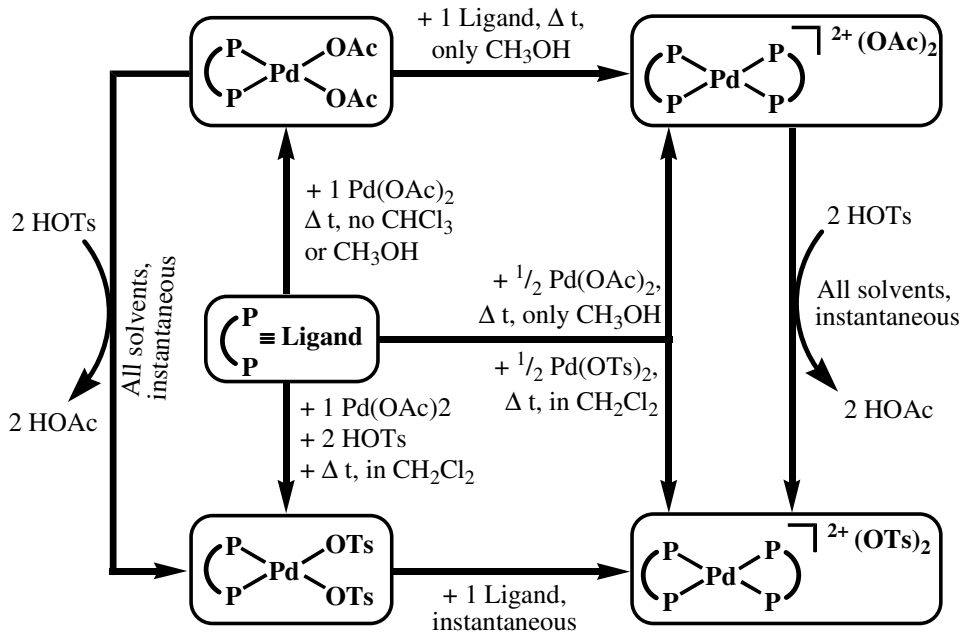

Figure 2.1. Schematic overview of the synthetic methods to form the monochelate complex [Pd(ligand)(anion)$_2$] or the bischelate complex [Pd(ligand)$_2$](anion)$_2$ with acetate or tosylate anions.

be synthesized; the other solvents are not polar enough to sufficiently dissociate the OAc^- anions. The bischelate complexes [Pd(ligand)$_2$](OTs)$_2$ can be prepared in all four solvents.

Not all complexes form instantaneously. Indeed, in some cases the desired complex is formed only after several hours (see complex formation studies for details). Therefore, depending on the ligand, the reaction mixture should stand for an appropriate amount of time (usually overnight), as otherwise a mixture of species may be isolated.

Once the monochelate or bischelate complex had been formed with the acetate anions, addition of two equivalents of *p*-toluenesulfonic acid resulted in the quantitative replacement of the anions in any of the solvents, as evidenced by the appearance of a peak around 1.0 ppm for acetic acid.
The 1,4-butyl bridged ligands present a special case. When applying the procedure of Mul and co-workers,[24] the unsubstituted ligand L4 yielded the monochelate complex. This was not the case for oMeO-L4 and oEtO-L4. When a

solution of $Pd(OAc)_2$ was added to oMeO-L4, a clear yellow solution was formed immediately. However, after standing for two minutes, a yellow precipitate formed, which turned red-brown over time. The isolated solid proved to be insoluble in a vast variety of different solvents, indicating that this solid is a coordination polymer. When a solution of $Pd(OAc)_2$ was added to oEtO-L4, a mixture of species was formed (several ^{31}P-resonances), which did not change over time. No attempts were made to further characterize these compounds.

Not all complexes were isolated and fully characterized; some were only detected in situ during the NMR studies. Nevertheless, for convenience, in Table S1 the proton and phosphorus resonances of all the palladium complexes that could be measured are summarized. The monochelate complexes are indicated as M(x)A or M(x)T with ligand x and coordinating acetate or tosylate anions, respectively, whereas the bischelate complexes are indicated as B(x)A or B(x)T with ligand x and non-coordinating acetate or tosylate anions.

2.2.2. Complex structures in the solid state

Light yellow transparent single crystals of the compounds $[Pd(oMeO\text{-}L2)(OAc)_2]$ (M(oMeO-L2)A), $[Pd(MeO\text{-}L3)(OAc)_2]$ (M(MeO-L3)A), $[Pd(MeO\text{-}L3X)(OAc)_2]$ (M(MeO-L3X)A), $[Pd(MeO\text{-}L3X^R)(OAc)_2]$ (M(MeO-L3X^R)A), and $[Pd(MeO\text{-}L3X)_2](OTs)_2$ (B(oMeO-L3X)T) were obtained using the solvent diffusion technique. The crystal structures were determined by X-ray diffraction; crystallographic data and details of the structure refinement are given in Table **2.2**. Perspective views of the molecular structures of M(oMeO-L3X)A and B(oMeO-L3X)T in the crystal are shown in Figure 2.2. Since the global structures of the monochelate complexes are very similar, projections of the complexes

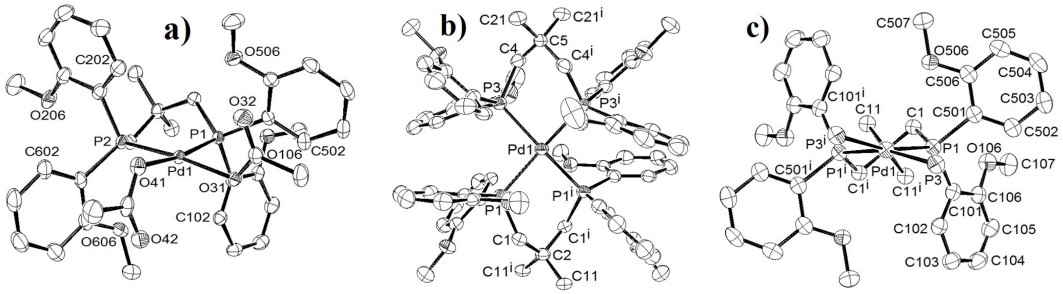

Figure 2.2. Displacement ellipsoid plots (50% probability level). a: $[Pd(oMeOL3X)(OAc)_2]$ (front view); b: cation of $Pd(oMeOL3X)_2](OTs)_2$ (top view); c: cation of $[Pd(oMeOL3X)_2](OTs)_2$ (front view along the twofold axis, one ligand omitted, except for the phosphorus atoms). Hydrogen atoms, uncoordinated anions and uncoordinated solvent molecules are omitted for clarity. Symmetry operation i: 1-*x*, *y*, 0.5-*z*.

M(oMeO-L2)A, M(oMeO-L3)A and M(oMeO-L3X^R)A can be found in the Supporting Information. Selected bond distances, angles and torsion angles are listed in

Table 2.2. Selected interatomic distances, angles, and other relevant geometric data for complexes M(oMeO-L2)A, M(oMeO-L3)A, M(oMeO-L3X)A, M(oMeO-L3X^R)A, and B(oMeO-L3X)T.

Complex:	**M(oMeO-L2)A***	**M(oMeO-L3)A**	**M(oMeO-L3X)A**	**M(oMeO-L3X^R)A**	**B(oMeO-L3X)T***	
	(pseudo) coordination [Å]					
$Pd_1 – P_1$	2.2177(6)	2.2223(6)	2.2366(6)	2.2341(8)	2.4091(8)	
$Pd_1 – P_2$		2.2273(5)	2.2305(5)	2.2254(8)		
$Pd_1 – P_3$					2.3938(9)	
$Pd_1 – O_{31}$	2.0984(14)	2.1112(14)	2.0891(13)	2.047(2)		
$Pd_1 – O_{41}$		2.0946 (13)	2.0936(15)	2.064(2)		
$Pd_1 – O_{32}$	2.9169(17)	2.8662(19)	3.1771(16)	3.099(2)		
$Pd_1 – O_{42}$		2.8067(19)	3.0718(16)	3.153(2)		
	*anagostic interactions [Å]***					
$Pd_1 \cdots H_{102}$	2.75	2.72	2.87	2.82	3.03	
$Pd_1 \cdots H_{202}$		2.69	2.75	2.71		
$Pd_1 \cdots H_{302}$					3.06	
	*C-H•••π interactions [Å]***					
$H_{502} \cdots C_{101}$	2.57	2.70	2.53	2.59	2.66	
$H_{502} \cdots C_{106}$	2.77	2.82	2.53	2.72	2.63	
$H_{602/702} \cdots C_{201/301}$		2.61	2.55	2.54	2.67	
$H_{602/702} \cdots C_{206/306}$		2.59	2.66	2.68	2.82	
	Angles [°]					
$P_3 – Pd_1 – P_{3'}$					86.04(3)	
$P_1 – Pd_1 – P_3$					95.71(3)	
$P_1 – Pd_1 – P_{3'}$					166.56(3)	
$P_1 – Pd_1 – P_{2/1'}$	85.98(3)	95.497(19)	90.62(2)	92.22(3)	85.69(4)	
$O_{31} – Pd_1 – O_{41/31'}$	92.22(8)	87.03(5)	92.20(6)	94.97(9)		
$P_1 – Pd_1 – O_{41}$	90.91(5)	90.78(4)	90.38(4)	87.00(6)		
$P_2 – Pd_1 – O_{42}$		87.14(4)	87.70(4)	86.24(6)		
$P_1 – Pd_1 – O_{41/31'}$	176.69(4)	174.80(4)	170.96(4)	172.80(6)		
$P_2 – Pd_1 – O_{31}$		171.72(4)	174.09(4)	176.36(6)		
$Pd_1 – O_{31} – C_{31}$	111.28(14)	108.29(13)	121.81(13)	117.90(18)		
$Pd_1 – O_{41} – C_{41}$		107.86(12)	117.96(14)	120.6(2)		
$Pd_1 – O_{32} – C_{31}$	73.80(14)	74.79(14)	68.60(12)	67.53(18)		
$Pd_1 – O_{42} – C_{41}$		75.65(14)	70.89(13)	68.40(18)		
	Dihedral angles between the PdP_2 and the PdX_2 planes [°]					
$PdP_2 – PdX_2$ (dihedral)	1.56(7), X = O	7.22(8), X = O	10.46(6), X = O	7.63(9), X = O	19.78(5), X = P	
	*Cremer-Pople ring puckering parameters for the PdP_2C_2 and PdP_2C rings****					
					Ring 1	Ring 2
Q_2 [Å]	0.492(2)	0.5247(19)	0.8588(17)	0.812(2)	0.906(3)	0.898(3)
Q_3 [Å]		0.3266(19)	-0.0369(16)	0.051(2)	0.000(2)	0.000(3)
θ [°]		58.09(18)	92.46(11)	86.42(14)	90.00(13)	90.00(19)
φ_2 [°]	270.00(12)	156.4(2)	266.99(11)	82.57(16)	270.00(14)	270.00(14)
	Torsion angles [°]					
$Pd_1 – P_1 – C_{101} – C_{102}$	-7.1(2)	-4.95(18)	-1.38(18)	11.5(3)	6.1(3)	
$Pd_1 – P_2 – C_{201} – C_{202}$		-5.67(19)	-1.8(2)	8.3(3)		
$Pd_1 – P_3 – C_{301} – C_{302}$					13.0(3)	
$Pd_1 – P_1 – C_{501} – C_{502}$	102.30(18)	-104.51(18)	105.15(18)	-113.0(3)	120.0(3)	
$Pd_1 – P_2 – C_{601} – C_{602}$		-102.44(17)	104.54(17)	-108.1(3)		
$Pd_1 – P_3 – C_{701} – C_{702}$					101.7(3)	

[*] Coordination rings are located on twofold axis. [**] Hydrogen atoms were introduced in calculated positions based on a C-H distance of 0.95 Å. [***] Cremer-Pople ring puckering parameters for the PdP_2C_2 and PdP_2C rings.[22]

Table **2.2**.
Complexes M(oMeO-L2)A and B(oMeO-L3X)T are located on twofold rotation axes, respectively, running through the palladium centre and the central carbon atom(s) of the ligand backbone. Hence, M(oMeO-L2)A has only one unique phosphorus atom, and B(oMeO-L3X)T only two. The palladium centers in the complexes M(oMeO-L2)A, M(oMeO-L3)A, M(oMeO-L3X)A, M(oMeO-L3X^R)A, and B(oMeO-L3X)T are in distorted square-planar geometries with *cis*-P_2O_2 donor sets for the monochelate complexes and a P_4 donor set for the bischelate complex. The Pd–P and Pd–O distances can be considered as normal.[26] Although the acetate anions are coordinated in a monodentate fashion, they may be considered pseudo-chelating with their second O-atom at distances to Pd ranging between 2.8067(19) (M(oMeO-L3)A) and 3.1771(16) (M(oMeO-L3X)A) Å, and Pd–O–C angles ranging between 67.53(18)° (M(oMeO-L3X^R)A) and 75.65(14)° (M(oMeO-L3X)A). The magnitude of the distortion from the ideal square-planar geometry varies considerably. The dihedral angle between the P–Pd–P and X–Pd–X (X = P or O) planes range from 1.56(7)° in M(oMeO-L2)A, to 7.22(8)-10.46(6)° in M(oMeO-L3)A, M(oMeO-L3X)A, and M(oMeO-L3X^R)A, and is 19.78(5)° in the bischelate complex B(oMeO-L3X)T. The large tetrahedral distortion in B(oMeO-L3X)T is due to the presence of large steric bulk of two ligands around the palladium centre; there are no other intermolecular or intramolecular contacts responsible for this distortion. The ligand bite angles also vary considerably. The ethylene bridged ligand oMeO-L2 in M(oMeO-L2)A has a bite angle of 85.98(3)°, whereas the propylene bridged ligand L7 in M(oMeO-L3)A has a bite-angle of 95.497(19)°. This angle is slightly compressed by the addition of steric bulk to the backbone, resulting in 90.62(2)° in M(oMeO-L3X)A and 92.22(3)° in M(oMeO-L3X^R)A. In the bischelate complex B(oMeO-L3X)T, the angle is compressed even further to a mere 85.69(4)°. The six-membered PdP_2C_2 coordination rings in M(oMeO-L3X)A, M(oMeO-L3X^R)A, and B(oMeO-L3X)T have a twist-boat and in M(oMeO-L3)A a screw-boat conformation, while the five-membered PdP_2C ring in M(oMeO-L2)A has a half-chair conformation.

It is possible to distinguish the two aryl rings on each phosphorus atom as oriented either axially (for the NMR discussion denoted as rings 100, 200, 300, and 400) or equatorially (rings 500, 600, 700, and 800) with respect to the chelate ring of the bidentate ligand (see for example rings 100 and 500 in Figure 2a and 2c). The axial phenyl rings are held in place by Pd···H interactions between its

ortho proton and the filled palladium d_z^2 orbital. Similar interactions have been reported for related nickel and palladium complexes.[27, 28] These interactions have been described as anagostic,[29] and are characterized by a Pd–P–C–C torsion angle close to 0°. The Pd···H distances (between 2.71 (M(oMeO-L3X^R)A) and 3.06 Å (B(oMeO-L3X)T)), and the Pd–P–C–C torsion angles (between 1.38(18)° (M(oMeO-L3X)A) and 11.5(3)° (M(oMeO-L3X^R)A)) of the observed anagostic interactions, can be considered as normal.[28] Furthermore, relatively strong intramolecular C-H···π interactions between the *ortho* protons of the equatorial rings (H502, H602, H702) and one π-bond of the axial rings (C101/C106, C201/C206, C301/C306) are observed.[30] The various H···C distances, ranging between 2.527 (for M(oMeO-L3X)A) and 2.817 (for M(oMeO-L3)A) Å, are well within the sum of the van der Waals radii of H and C (2.90 Å).

The structures of the complexes [Pd(L2)OAc$_2$],[31] [Pd(oMeO-L2)Cl$_2$] and [Pd(oMeO-L3)Cl$_2$],[32] as well as of the analogous nickel^{II} complexes [Ni(oMeO-L3)I$_2$][27] and [Ni(oMeO-L3)Cl$_2$][33] have been published; the reported distances, angles and Pd···H or Ni···H interactions are comparable to those described above.

2.2.3. Complex structures in solution

As typical examples, the ^{1}H-NMR-spectra of the monochelate complexes M(oMeO-L3X^R)A and M(oMeO-L3X^R)T are shown in Figure 2.3a and 2.3c respectively (in $(CD_3)_2CO$)). In the solid-state structures, the two phenyl rings on each phosphorus atom are distinct with respect to their orientation to the plane of coordination and have been labelled as axial or equatorial. In solution at room temperature, however, only one set of resonances is observed, as is shown in Figure 2.3a for M(oMeOL3X^R)A. The observation that the two phenyl rings appear to be equivalent in solution is due to dynamic flipping of the backbone.[27] When this flipping is frozen at low temperature, the axial and equatorial protons become inequivalent; two sets of proton resonances are observed in ^{1}H-NMR spectra (Figure 2.3b). The proton resonances of the axial phenyl rings are relatively deshielded due to the Pd···H interactions, whereas the proton resonances of the equatorial phenyl rings are shielded due to the H···Cπ interactions.

For the monochelate complex M(oMeO-L3X^{R})T with the weakly-coordinating OTs^{-} anions (Figure 2.3c) a different phenomenon is observed upon cooling; the peaks are not split, but broadened (Figure 2.3d). It suggests that the weakly-coordinating OTs^{-} anions are displaced with solvent molecules; the Pd^{II} ion is in a [Pd(ligand)(solvent)$_2$]$^{2+}$ coordination sphere and even at low temperatures the coordinated solvent ligands are quickly exchanged with other solvent molecules, thus decreasing the steric hindrance for the flipping of the backbone. Further cooling should result in a complete splitting into two sets of protons. In contrast, the presence of relatively strongly coordinating OAc^{-} anions in M(oMeO-L3X^{R})A makes the overall complex more rigid at lower temperature, thereby hindering the dynamic flipping of the backbone. In the case of the crowded [Pd(ligand)$_2$](anion)$_2$ complexes, two sets of proton resonances are observed at all temperatures. Their spectra resemble the one shown in Figure 2.3b.

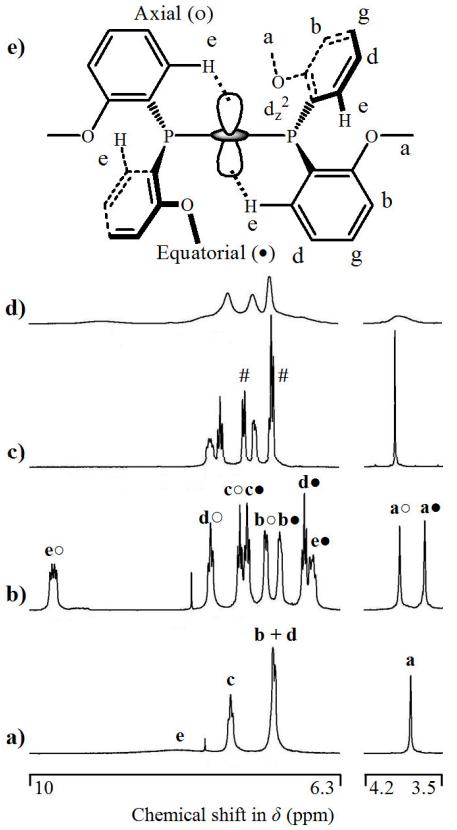

Figure 2.3. ^{1}H-NMR spectra of monochelate complexes in $(CD_3)_2CO$: a) M(oMeO-L3X^{R})A at 23 °C; b) M(oMeO-L3X^{R})A at –60 °C; c) M(oMeO-L3X^{R})T at 23 °C; d) M(oMeO-L3X^{R})T at –60°C; e) schematic view of the interactions and labeling of the H atoms. An '●' indicates that the resonance belongs to an equatorially aligned ring, 'o' indicates that the resonance belongs to an axially aligned ring, and '#' indicates a resonance from a tosylate anion.

2.2.4. Complex formation studies

2.2.4.1 General

NMR-studies were performed to explore the kinetics of formation of the palladium complexes of different types of ligands in more detail. Using $Pd(OAc)_2$, the complex formation was studied in the deuterated solvents CD_2Cl_2, $(CD_3)_2CO$, and CD_3OD. When using $Pd(OTs)_2$ the only suitable solvent is a

Table 2.3. Overview of complex formation studies, monitored with ^{1}H and ^{31}P NMR spectroscopy.[a]

Entry	Ligand	$Pd(OAc)_2$ CD_3OD	$Pd(OAc)_2$ $(CD_3)_2CO$	$Pd(OAc)_2$ CD_2Cl_2	$Pd(OTs)_2$ CD_2Cl_2[b]
1	L2	b→m (0.44)	m	m	(b in CD_3OD)[9]
2	oMeO-L2	m + b	m	m	
3	oEtO-L2	m + b	m	m	
4	L3	m	m	m	b→m (6.23)
5	L3X	m	m	m	
6	oMe-L3	i	p→m (1.03)	m	
7	oMeO-L3	p→m (0.07)[b]	p→m (0.49)	p→m (0.53)	b→m (0.01)[c]
8	oEtO-L3	i	p→m (0.25)	p→m (1.00)	
9	pMeO-L3	m	m	m	
10	oMeO-L3X	m	m	m	
11	oMeO-L3X^2	m	m	m	
12	oEtO-L3X^2	m	m	m	
13	oMeO-L3X^R	i	m	m	
14	L4			p→m (1.07)	m
15	oMeO-L4	i	i	p→x (1.26)	
16	oEtO-L4	i	i	p→x (0.58)	
17	pMeO-L4			p→m (1.15)	
18	L4X			m	
19	oMeO-L4X			m	

[a] $[Pd(OAc)_2]$ or [Ligand] = 16 mM. The values between parentheses represent a reaction constant (k' in h^{-1}, see experimental section) for the observed conversion. m = monochelate complex; b = bischelate complex; p = polynuclear complex; x = unidentified complex(es); i = ligand or complex is insoluble. See text for further explanation. [b] 17% ($^{v}/_{v}$) of $(CD_3)_3CO$ in CD_2Cl_2 was actually used due to solubility problems. [c] the complex formation was accompanied by plating over time.

mixture of $(CD_3)_2CO$ in CD_2Cl_2 (17% *v/v*); $Pd(OTs)_2$ is immediately reduced in CD_3OD, HOTs and $Pd(OTs)_2$ are insoluble in pure CD_2Cl_2, and most $[Pd(ligand)_2](OTs)_2$-type complexes are insoluble in $(CD_3)_2CO$. An overview of the results of selected complex formation studies is presented in Table 2.3. During these studies a variety of complexes were observed *in situ*, but were not isolated. Nonetheless, an overview of the ^{1}H- and ^{31}P-NMR data of all the detected complexes is given in Appendix I.

2.2.4.2. Ethylene-bridged ligands

Use of the ethylene-bridged ligands (L2, oMeO-L2, and oEtO-L2) directly results in the formation of the monochelate complex [Pd(ligand)(OAc)2] when the reaction is performed in $(CD_3)_2CO$ or CD_2Cl_2 (entries 1-3). In CD_3OD however, as reported by Mul and co-workers,[24] L2 initially forms the bischelate complex (δ_P = 58.7 ppm) as the kinetic product, which converts to the thermodynamically

more stable monochelate complex (δ_P = 63.7 ppm) over time (k' = 0.44 h^{-1}). In the case of the sterically more demanding ligands oMeO-L2 and oEtO-L2, in CD_3OD the monochelate complex is formed directly as the major species (~ 70%). The other product is the bischelate complex (~ 30%). The composition of this mixture did not change over time (eight hours), nor upon addition of another 0.2 equivalents of $Pd(OAc)_2$. This indicates that the oMeO moieties on the ligand shield the palladium in the bischelate complex from OAc^- coordination. It thus appears that ethylene-bridged ligands directly form the monochelate complex, except in a relatively polar solvent. Only then the OAc^- anions may dissociate from Pd^{II} to allow a second ligand to coordinate, thus forming the bischelate complex. Indeed, it has been reported that by employing the weakly-coordinating OTs^- anions, the bischelate complex is formed exclusively.[24]

2.2.4.3. Propylene-bridged ligands

For the ligands with an unsubstituted propylene backbone (entries 4 and 6-9) different behaviour is observed when starting from $Pd(OAc)_2$. In the case of L3, the monochelate complex is formed immediately in all solvents. However, the *ortho*-methoxy analogue of this ligand (oMeO-L3) forms the monochelate complex *via* an intermediate species, as is illustrated in Figure 2.4 (in CD_2Cl_2).

This intermediate is not the usual bischelate complex, since the characteristic resonances of the axial and equatorial (*ortho*) protons are not observed. In the NMR spectra of this intermediate, no free ligand ^{31}P resonance is observed at −37 ppm, and several resonances are observed for the *ortho*-methoxy protons (3.3 – 3.9 ppm). The resonances around 1.8 and 0.6 ppm are indicative of different types of OAc^- anions. These observations suggest the formation of a polynuclear species, which could be either a polymeric compound $[Pd(oMeO\text{-}L3)(OAc)_2]_n$ in which the ligand is monodentate and bridging, or a dinuclear complex $[\{Pd(oMeO\text{-}L3)(OAc)\}_2(oMeO\text{-}L3)](OAc)_2$. The intermediate species could be isolated, but a mass higher than that of the monochelate complex could not be detected using ESI mass spectroscopy.

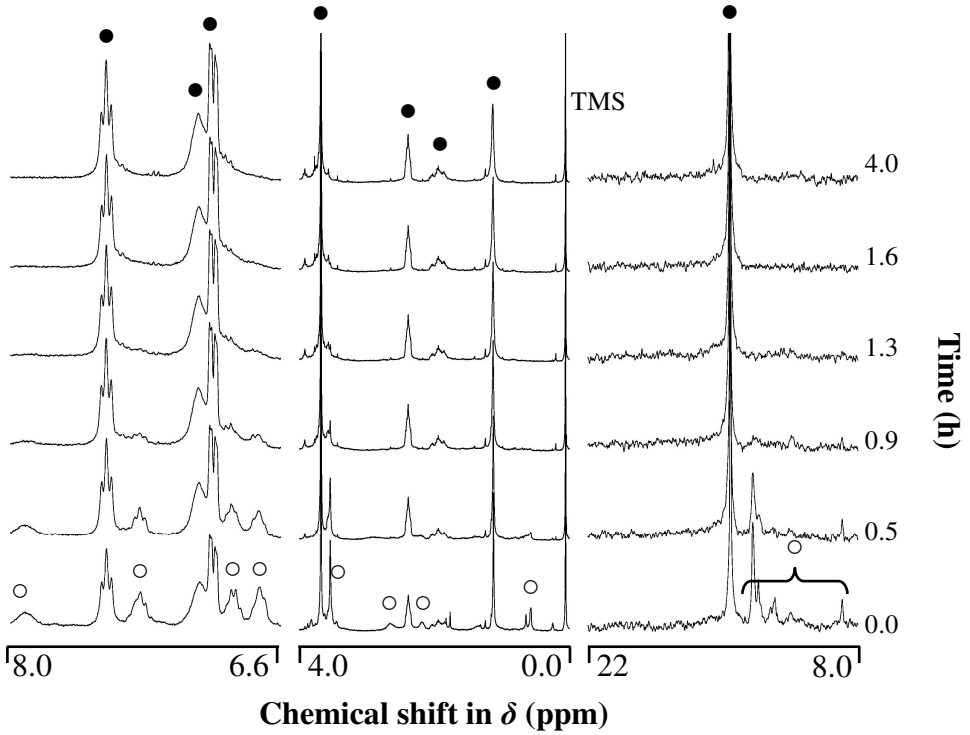

Figure 2.4. Complex-forming study followed by ^{1}H- and ^{31}P-NMR; [Pd(OAc)$_2$] in CD_2Cl_2 added to **oMeO-L3**. ● = resonance of the (thermodynamic) monochelate complex; ○ = resonance of the (kinetic) intermediate.

To investigate whether the difference in behaviour of the ligands L3 and oMeO-L3 is due to steric or electronic reasons, a series with increased steric bulk on the *ortho* position was studied; L3 (H), oMe-L3 (Me), oMeO-L3 (MeO), and oEtO-L3 (EtO). The same type of intermediate is observed for these ligands (entries 6-8) in $(CD_3)_2CO$; the conversion to the monochelate complex follows approximate first-order kinetics (see Figure 2.5). An increase in steric bulk results in a lower p → m conversion rate, with *k'* = 1.03, 0.49, and 0.25 h^{-1} for oMe-L3, oMeO-L3, and oEtO-L3, respectively. Apparently, in the proposed intermediate polynuclear species, the larger steric '*ortho*-bulk' of the ligand shields the palladium d_z^2 orbital (see also Figure 2.3e) for the approach of a phosphane (in the case of [Pd(L)(OAc)$_2$]$_n$) or an acetate anion (in the case of [{Pd(L)(OAc)}$_2$L](OAc)$_2$).

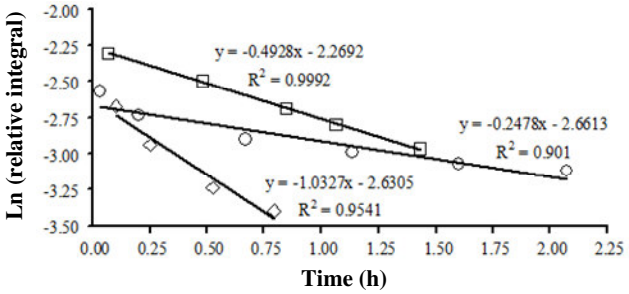

Figure 2.5. Effect of the steric bulk on monochelate complex formation with propylene-bridged ligands in acetone; Plot of ln(relative integral) versus time (h), at 23 °C with linear trend lines. ◇ = oMe-L3 @ δ = 8.1 ppm; ○ = oEtO-L3 @ δ = 7.4 ppm; □ = oMeO-L3 @ δ = 7.3 ppm.

This is illustrated in Figure 2.6. To confirm that the effect is purely based on sterical grounds the experiment was repeated with pMeO-L3 (entry 9). This ligand indeed showed the immediate formation of the monochelate complex in all three solvents.

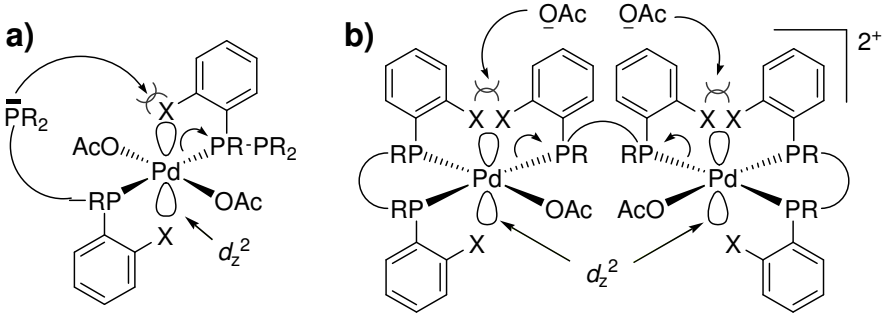

Figure 2.6. Illustration of the ligand induced steric hampering that retards the formation of [Pd(**L**)(OAc)$_2$]–type complexes. The steric bulk of the *ortho*-moieties (X) of the ligand shields the palladium d_z^2 orbital from ligand approach in [Pd(L)(OAc)$_2$]$_n$ (a), or from acetate coordination in [{Pd(L)(OAc)}$_2$(L)](OAc)$_2$ (b).

Interestingly, when the propylene backbone is more rigid by the *gem*-dialkyl substitution of the central carbon atom in the bridge (oMeO-L3X, oMeO-L3X^2 oEtO-L3X^2, and oMeO-L3X^R, entries 10-13), no intermediate species is observed. In these cases the monochelate complex is immediately formed, even for ligand oEtO-L3X^2, which comprises the larger oEtO substituent on the phenyl rings. This observation is attributed to the so-called 'Thorpe-Ingold' effect;[34, 35] due to

the presence of the two substituents on the central carbon atom in the backbone, the two phosphorus atoms are pre-oriented and more likely to form a chelate on palladium. In line with this, L3X also forms the monochelate complex immediately.

2.2.4.4. Butylene-bridged ligands

With the butylene-bridged ligands L4 and pMeO-L4 (entries 14 and 17) the monochelate complex is formed only *via* an intermediate species; several ^{31}P resonances around 12 ppm disappear over time. The approximate first order reaction constants of these conversions are of the same magnitude (in CD_2Cl_2 *k'* = 1.07 and 1.15 h^{-1} for L4 and pMeO-L4, respectively). This difference in behaviour between the unsubstituted C3 and C4-bridged ligands is ascribed to the increased

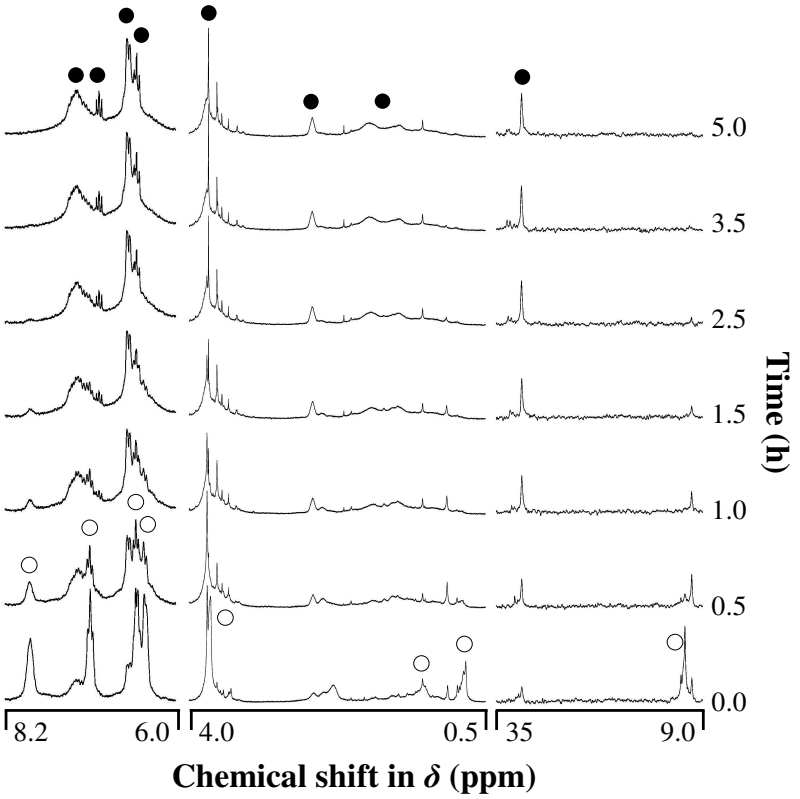

Figure 2.7. Complex formation for oMeO-L4 monitored by ^{1}H- and ^{31}P-NMR; $[Pd(OAc)_2]$ in CD_2Cl_2 added to oMeO-L4. ● = resonance of thermodynamic product; ○ = resonance of the kinetic intermediate.

flexibility of the butylene backbone. This renders the ligand a weaker chelate thus favoring the initial formation of a polynuclear species. In agreement with this hypothesis, using a ligand with a more rigid backbone (L4X, entry 18) the monochelate complex is formed immediately.

A different thermodynamic species is observed when steric bulk is added to the *ortho* position in the flexible butylene-bridged ligands (oMeO-L4 and oEtO-L4). This is exemplified for ligand oMeO-L4 in Figure 2.7. The kinetic product is rather similar to those formed for L4 (*o*-H4) and pMeO-L4 analogues. A number of resonances is observed in ^{31}P NMR around 11 ppm, and in ^{1}H NMR around 3.75 ppm for the methoxy group. Especially the aromatic resonance around 7.9 ppm is very characteristic for this type of intermediate. However, for oMeO-L4 and pMeO-L4 the nature of the thermodynamic product is unclear; it is most certainly not the desired monochelate complex, or the bischelate complex. The rate of conversion again depends on the size of the steric bulk; k' = 1.26 (oMeO-L4) and 0.58 (oEtO-L4). Since pMeO-L4 eventually forms the monochelate complex, the formation of the unidentified species is ascribed to steric influences. When the backbone is made more rigid (oMeO-L4X), the monochelate complex is formed immediately and none of the other species were detected.

2.2.4.5. The role of the coordinating strength of the anions

Not only the steric bulk and (the rigidity of) the ligand backbone are important for the course and rate of the complex formation. The coordination strength of the anions was also found to be an important factor. For L2 (ethylene backbone) it is known that when employing the weakly coordinating $CF_3C(O)O^-$ anions in CD_3OD, the bis-chelate complex is both the kinetic and thermodynamic species.[24]

For the propylene bridged ligands, it was found that the more polar the solvent, the more dissociated the OAc^- anions become, and hence the slower the conversion to the monochelate complex. This is most prominently reflected in the series performed with oMeO-L3. As can be seen from entry 7 in Table 2.3, the monochelate complex is formed more rapidly in CD_2Cl_2 (k' = 0.53) than in $(CD_3)_2CO$ (k' = 0.49), and only very slowly in CD_3OD (k' = 0.07). Similar trends were observed with ligands oMe-L3 and oEtO-L3 (entries 6 and 8). That these

observations are due to the coordinating ability of the anions is confirmed by employing weakly-coordinating OTs^- anions. Instead of a polynuclear species, oMeO-L3 now forms the bischelate complex as kinetic product (entry 7). Evidently, OTs^- anions are highly dissociated (even in the relatively apolar CD_2Cl_2) to allow the formation of a cationic species with a P_4 donor set. The conversion to the monochelate complex is extremely slow (k' = 0.01 h^{-1}), because the oMeO moieties shield the palladium d_z^2 orbitals from anion coordination (see Figure 2.6). Evidently, OTs^- anions coordinate so weakly that they can hardly overcome this steric repulsion induced by the oMeO moieties. When working with L3 (*o*-H, entry 4), the bischelate complex was also formed as intermediate. However, due to the smaller *ortho*-bulk the conversion to the monochelate complex proceeds very rapidly (k' = 6.23 h^{-1}).

The coordinating ability of the anions also influences the course of the complex formation with butylene-bridged ligands. As can be seen in entry 14 (L4, *o*-H), when employing OTs^- anions the monochelate complex is formed immediately, whereas with OAc^- anions it proceeds *via* some intermediate. This can be rationalized as follows. When OAc^- anions are used, the monochelate complex (P_2O_2 donor set) is formed *via* a PO_3 donor set. This is due to the strongly-coordinating nature of the OAc^- anions (perhaps in a bridging manner). When the anions are weakly-coordinating (OTs^-) the P_2O_2 donor set is formed immediately. That the ligand L4 does not form the bischelate complex (e.g., a P_4 donor set like its propylene bridged analogue L3) is ascribed to its larger bite-angle ($\beta \approx 99°$ *versus* 94°).[36] This imposes a sterical constraint on the adjacent coordination sites,[37, 38] thus disfavouring bischelate complex formation.

2.3. Conclusions

A variety of palladium complexes with substituted bidentate diphenylphosphane ligands has been synthesized using straightforward synthetic procedures. More specifically, monochelate and bischelate complexes with strongly (OAc^-) or weakly (OTs^-) coordinating anions have been obtained, and structures of representative complexes have been described. Using variable temperature NMR studies it was shown that the solid state structure of this type of complexes is fully retained in solution.

It was shown that three ligand-dependent factors play a crucial role in the formation of [Pd(ligand)(anion)$_2$]-type complexes: the length of the bridge between the phosphorus donors; the steric bulk at the *ortho* position of the phenyl rings; and the rigidity of the backbone. The coordinating ability of the anions was also found to be an important factor in the complex forming process.

Depending on these factors, the desired [Pd(ligand)(anion)$_2$] complex is formed instantaneously, *via* some intermediate, or not at all. Notably, when making the ligand bridge more rigid, the desired [Pd(ligand)(anion)$_2$] complex is formed directly in all cases studied.

It is thus concluded that it is important to realize that the formation of [Pd(ligand)(anion)$_2$]-type complexes is not always instantaneous or successful. Thus, when performing catalytic reactions with *in situ* formed complexes, one should make sure that the desired complex will actually form. With this study I hope to have provided a significant contribution to the fundamental understanding which ligand parameters determine whether the desired catalyst will indeed be formed.

2.4. Experimental Section

2.4.1. Materials

Solvents and chemicals were commercially available as A.R. grade and used as received, unless stated otherwise. The ligand and complex syntheses were performed under an inert atmosphere of argon and the purifications were commonly performed in air, unless stated otherwise. A schematic overview of the ligands used in this study is presented in Table 2.1. The ligands L2, L3, L4, and pMeO-L4 are commercially available and were used as received. The ligands L3X, oMeO-L4, and oEtO-L4 have been synthesized according to literature procedures.[39-42] The other ligands were obtained as a gift from Shell International Chemicals B.V., where they were prepared according to literature procedures.[43-51] All ligand molecular data are summarized in Appendix I.

2.4.2. Physical methods

Common analytical techniques

^{1}H- and ^{31}P{^{1}H}-NMR spectra were recorded using a DPX Bruker instrument operating at 300 or 400 MHz. Chemical shifts are reported in δ (parts per million); the proton resonances are given relative to the solvent peak (CD_3OD = 3.33, $(CH_3)_2SO$ = 2.50, $(CH_3)_2CO$ = 2.06, $CDCl_3$ = 7.26, CD_2Cl_2 = 5.30 ppm) or tetramethylsilane (TMS, 0 ppm). The phosphorus resonances are given relative to the external standard H_3PO_4 (85%, 0 ppm). C, H, and N analyses were carried out using an automatic Perkin-Elmer 2400 Series II CHNS/O microanalyzer. ESI Mass Spectroscopy was carried out using a Finnigan Aqua Mass Spectrometer equipped with an electrospray ionisation (ESI) source. Sample solutions (10 μL of a 1 mg/mL solution) were introduced in the ESI source by using a Dionex ASI-100 automated sampler injector and an eluent running at 0.2 ml/min.

X-ray crystal structure determinations

X-ray intensities were measured on a Nonius KappaCCD diffractometer with rotating anode (graphite monochromator, λ = 0.71073 Å) at a temperature of 150(2) K. Data were integrated with the HKL2000[52] ([Pd(oMeO-L2)$(OAc)_2$], [Pd(oMeO-L3X)$(OAc)_2$], [Pd(oMeO-L3X)]$(OTs)_2$) or EvalCCD[53] ([Pd(oMeO-L3)$(OAc)_2$], [Pd(oMeO-L3X^{R})$(OAc)_2$]) software. The structures were solved with Direct Methods using the programs SIR-97[54] ([Pd(oMeO-L2)$(OAc)_2$], [Pd(oMeO-L3X)]$(OTs)_2$) and SHELXS-97[55] ([Pd(oMeO-L3X)$(OAc)_2$]) or with automated Patterson Methods using the program DIRDIF-99[56] ([Pd(oMeO-L3)$(OAc)_2$], [Pd(oMeO-L3X^{R})$(OAc)_2$]). The structures were refined with SHELXL-97[55]. Non-hydrogen atoms were refined with anisotropic displacement parameters. Hydrogen atoms were located in difference-Fourier maps ([Pd(oMeO-L2)$(OAc)_2$], [Pd(oMeO-L3X)$(OAc)_2$]) or introduced in calculated positions ([Pd(oMeO-L3)$(OAc)_2$], [Pd(oMeO-L3X^{R})$(OAc)_2$], [Pd(L10)]$(OTs)_2$) and refined with a riding model. Drawings, structure calculations and checking for higher symmetry were performed with the PLATON software[57]. Further experimental details are given in Table 2.4.

CCDC 748839-748843 contain the supplementary crystallographic data for this chapter. These data can be obtained free of charge from The Cambridge Crystallographic Data Centre via www.ccdc.cam.ac.uk/data_request/cif.

[Pd(oMeO-L2)$(OAc)_2$]: The $CHCl_3$ solvent molecule was refined with a disorder model. [Pd(oMeO-L3)$(OAc)_2$]: Hydrogen atoms of the water molecule were refined freely with isotropic displacement parameters. [Pd(oMeO-L3X)$(OAc)_2$]: Hydrogen atoms of the water molecules were kept fixed at the positions located in difference Fourier maps. The methyl groups of the acetate ligands were refined with two conformations, respectively. [Pd(oMeO-L3X)]$(OTs)_2$: The crystal structure contains solvent accessible voids (1046 $Å^3$ / unit cell) filled with disordered solvent molecules. Their contribution to the structure factors was secured by back-Fourier transformation using the SQUEEZE routine of the program PLATON[57] resulting in 307 e^- / unit cell.

Table 2.4. Details of the X-ray crystal structure determinations.

complex formula	[Pd(oMeO-L2)$(OAc)_2$]	[Pd(oMeO-L3)$(OAc)_2$]	[Pd(oMeO-L3X)$(OAc)_2$]	[Pd(oMeO-L3X^R)$(OAc)_2$]	[Pd(oMeO-L3X)$_2$]$(OTs)_2$
CCDC refcode	748839	748840	748841	748842	748843
emperical formula	$C_{34}H_{38}O_8P_2Pd \cdot 2CHCl_3$	$C_{35}H_{40}O_8P_2Pd \cdot H_2O$	$C_{37}H_{44}O_8P_2Pd \cdot 3H_2O$	$C_{43}H_{52}O_{10}P_2Pd$	$[C_{66}H_{76}O_8P_4Pd](C_7H_7O_3S)_2$
fw	981.72	775.03	839.11	897.19	1569.92
crystal colour	colourless	yellow	colourless	yellow	yellow
crystal size [mm^3]	0.21x0.15x0.12	0.24x0.18x0.15	0.30x0.12x0.08	0.66x0.12x0.12	0.30x0.12x0.12
crystal system	monoclinic	monoclinic	monoclinic	monoclinic	monoclinic
space group	C2/c (no. 15)	$P2_1/c$ (no. 14)	$P2_1/c$ (no. 14)	$P2_1/c$ (no. 14)	C2/c (no. 15)
***a* [Å]**	21.3571(2)	13.9845(3)	13.7552(1)	10.8518(4)	26.4819(3)
***b* [Å]**	11.0576(1)	16.2664(4)	14.2919(1)	26.8681(11)	14.1198(2)
***c* [Å]**	19.5445(2)	20.0199(3)	20.0689(2)	15.5000(7)	24.7120(3)
β [°]	116.1887(4)	130.991(2)	96.4044(4)	113.881(3)	118.1165(6)
***V* [Å^3]**	4141.78(7)	3437.47(16)	3920.68(6)	4132.4(3)	8149.85(18)
Z	4	4	4	4	4
d_{calc} [g/cm^3]	1.574	1.498	1.422	1.442	1.279
μ [mm^{-1}]	0.961	0.687	0.612	0.584	0.417
(sin θ/λ)$_{max}$ [Å^{-1}]	0.65	0.65	0.65	0.65	0.60
refl. (meas./unique)	33907 / 4746	58871 / 7906	55912 / 8984	136182 / 9451	37289 / 7346
abs. corr.	multi-scan	multi-scan	multi-scan	multi-scan	multi-scan
abs. corr. range	0.85-0.89	0.75-0.90	0.92-0.96	0.60-0.93	0.74-0.96
param. / restraints	270 / 66	438 / 0	470 / 0	511 / 0	464 / 0
***R*1/*wR*2 [*I*>2σ(*I*)]**	0.0299 / 0.0731	0.0257 / 0.0579	0.0314 / 0.0722	0.0409 / 0.0745	0.0463 / 0.1129
***R*1/*wR*2 [all refl.]**	0.0436 / 0.0793	0.0400 / 0.0637	0.0470 / 0.0797	0.0676 / 0.0856	0.0685 / 0.1222
S	1.100	1.044	1.067	1.152	1.031
$\Delta\rho_{min/max}$ [eÅ^{-1}]	-0.54 / 0.51	-0.43 / 0.60	-0.68 / 0.84	-0.71 / 0.57	-0.59 / 0.95

2.4.3. NMR complex formation studies

Preparation of the samples, using $Pd(OAc)_2$

12.8 μmol of the ligand was weighed into an NMR tube and put under argon. In another tube, 3.59 mg (16 μmol) of $Pd(OAc)_2$ was dissolved in 1 ml of solvent under an argon atmosphere. Of this solution, 0.8 ml (12.8 μmol of Pd) was added to the ligand using a 1 ml syringe, which was dry and flushed with argon. The thus obtained mixture (16 mM) was thoroughly mixed using a vortex mixer

until a clear solution was obtained. When no clear solution was obtained within ten minutes of mixing, the sample was considered to be insoluble and was discarded.

Preparation of the samples, using $Pd(OTs)_2$

12.8 μmol of the ligand was weighed into an NMR tube and put under argon. In another tube, 3.59 mg (16 μmol) $Pd(OAc)_2$ and 5.51 mg (32 μmol) HOTs were dissolved in 1 ml $(CD_3)_2CO$ in CD_2Cl_2 (17% v/v), under an argon atmosphere. Of this solution, 0.8 ml (12.8 μmol of Pd) was added to the ligand using a 1 ml syringe, which was dry and flushed with argon. The thus obtained mixture (16 mM) was thoroughly mixed using a vortex mixer until a clear solution was obtained. When no clear solution was obtained within ten minutes of mixing, the sample was considered to be insoluble and was discarded.

NMR kinetic measurements

The clear solutions were monitored with ^{1}H- and ^{31}P{^{1}H}-NMR spectroscopy, over a period of about four to fourteen hours. All measurements of the same experiment (e.g. a specific complex formation study) were recorded with an identical number of free inductive decays (FIDs). For a typical proton measurement, the number of FIDs was 16. For the phosphorus NMR spectra the number of FIDs was typically 40.

Data Analysis

For the data analysis of the complex formation studies, the integral of an isolated aromatic resonance of the intermediate species was taken relative to the total integral of all aromatic protons. The natural logarithm of this number was plotted against time, which always resulted in a hyperbolically shaped curve. Of the initial linear part, the best fit was calculated with the least-squares method. These are the graphs that are given in this paper. The slopes of these linear functions reflect the (presumed first order) reaction constant (*k*'), not in absolute, but in relative sense. This was done because the exact nature of the disappearing species is (in most cases) unknown.

Low temperature NMR experiments

Some of the obtained complexes were characterized by ^{1}H- and ^{31}P-NMR spectroscopy, both at room temperature (20 °C) and at low temperature (–60 °C). This was typically done by monitoring the ^{1}H- and ^{31}P-NMR resonances of a 16 mM solution during cooling at 20, 0, –20, –40, and –60 °C. Before a spectrum at a specific temperature was recorded, it was ensured that the cooling apparatus was stable with an error of about 1 °C. When this was achieved, a waiting period of about ten minutes was applied to ensure that the sample had acquired the temperature as indicated by the cooling apparatus.

2.4.4. General methods for the synthesis of the complexes

Method A. For [Pd(Ligand)$(OAc)_2$]

A 74 mM solution of $Pd(OAc)_2$ in CH_2Cl_2 was prepared and filtered. A 25 ml round-bottomed flask filled with argon was charged with 10 ml of this solution and a magnetic stirring rod. To the stirred solution, 0.74 mmol of the solid ligand was added and the reaction mixture was stirred overnight (wrapped in aluminium foil), where after the solvent volume was reduced to about 5 ml. The complex was precipitated with Et_2O/*n*-hexane, collected by filtration over a glass frit (P4), washed with Et_2O/*n*-hexane and dried *in vacuo*.

Method B. For [Pd(Ligand)(OTs)$_2$]

A 74 mM solution of $Pd(OAc)_2$ in CH_2Cl_2 was prepared and filtered. A 25 ml round-bottomed flask filled with argon was charged with 10 ml of this solution and a magnetic stirring rod. To the stirred solution, 0.74 mmol of the solid ligand was added and the reaction mixture was stirred overnight (wrapped in aluminium foil). Then, *para*-toluene sulfonic acid (1.5 mmol, 0.26 g) was added and the solvent volume was reduced to about 5 ml. The complex was precipitated with Et_2O/*n*-hexane, collected by filtration over a glass frit (P4), washed with Et_2O/*n*-hexane and dried *in vacuo*.

Method C. For [Pd(Lidand)$_2$](OAc)$_2$

A 25 ml round-bottomed flask filled with argon was charged with 15 ml MeOH, 1 mmol of the ligand, and a stirring rod. The resulting suspension was stirred, and 2 ml of a filtered $Pd(OAc)_2$ solution (0.25 M in CH_2Cl_2) was added. After overnight stirring (wrapped in aluminium foil), the solvent volume was reduced to about 5 ml. The complex was precipitated with Et_2O/*n*-hexane, collected by filtration over a glass frit (P4), washed with Et_2O/*n*-hexane and dried *in vacuo*.

Method D. For [Pd(Ligand)$_2$](OTs)$_2$

A 25 ml round-bottomed flask filled with argon was charged with 15 ml MeOH, 1 mmol of the ligand, and a stirring rod. In another round-bottomed flask, 2 mmol (0.35 g) of *para*-toluene sulfonic acid was added to 4 ml of a 0.25 M solution of $Pd(OAc)_2$ in CH_2Cl_2. From this solution, 2 ml were added to the ligand/MeOH suspension. After overnight stirring (wrapped in aluminium foil), the solvent volume was reduced to about 5 ml. The complex was precipitated with Et_2O/*n*-hexane, collected by filtration over a glass frit (P4), washed with Et_2O/*n*-hexane and dried *in vacuo*.

2.4.5. Complex data

[Pd(L2)(OAc)$_2$] (M(L2)A) was prepared following method A. The product was obtained as a yellow powder, with an isolated yield of 97% (447 mg). The compound was recrystallized by layering a solution of the complex in dichloromethane with diethyl ether. ^{1}H NMR (300 MHz, CH_3OH): δ 7.80 (q, 8H, *m*-Ph-*H*), 7.52 (m, 4H, *p*-Ph-*H*), 7.45 (t, 8H, *o*-Ph-*H*), 2.50 (m, 4H, PCH_2), 1.49 (s, 6H, OC(O)CH_3) ppm; ^{31}P NMR (300 MHz, CH_3OH): δ 63.66 ppm. Elemental analyses for [Pd(L2)(OAc)$_2$], $C_{30}H_{30}O_4P_2Pd$ (622.92) • 0.75 CH_2Cl_2: calcd. C 53.79, H 4.62; found C 53.58, H 4.65. ESI Mass Spectroscopy, m/z found (calcd): $[M^- OAc]^+$ = 562.66 (563.05).

[Pd(L2)(OTs)$_2$] (M(L2)T) was prepared following method B. The product was obtained as a yellow powder, with an isolated yield of 89% (558 mg). The compound was recrystallized by layering a solution of the complex in dichloromethane with *n*-hexane. ^{1}H NMR (300 MHz, $OC(CH_3)_2$): δ 7.95 (q, 8H, *m*-Ph-*H*), 7.76 (m, 4H, *p*-Ph-*H*), 7.63 (m, 8H, *o*-Ph-*H*), 7.51 (d, 4H, *o*-OTs-*H*), 7.11 (d, 4H, *m*-OTs-*H*), 3.08 (m, 4H, PCH_2), 2.32 (s, 6H, *p*-OTs-CH_3) ppm; ^{31}P NMR (300 MHz, $OC(CH_3)_2$): δ 74.26 ppm. Elemental analyses for [Pd(L2)(OTs)$_2$], $C_{40}H_{38}O_6P_2PdS_2$ (847.22) • 0.5 CH_2Cl_2 • 0.25 C_6H_{14}: calcd. C 54.24, H 5.08, S 5.88; found C 54.24, H 5.00, S 5.91. ESI Mass Spectroscopy, m/z found (calcd): $[M - OTs]^+$ = 674.70 (675.05).

[Pd(L2)$_2$](OTs)$_2$ (B(L2)T) was prepared following method D. The product was obtained as a yellow powder, with an isolated yield of 92% (573 mg). The compound was recrystallized by layering a solution of the complex in dichloromethane with *n*-hexane. ^{1}H NMR (300 MHz, $CHCl_3$): δ 8.08 (d, 4H, *o*-OTs-*H*), 7.46 (m, 20H, *m*-Ph-*H* + *m*-OTs-*H*), 7.26 (m, 20H, *o*-Ph-*H* + *p*-Ph-*H*), 3.16 (m, 8H, PCH_2), 2.39 (s, 6H, *p*-OTs-CH_3) ppm; ^{31}P NMR (300 MHz, $CHCl_3$): δ 56.74 ppm. Elemental analyses for [Pd(L2)$_2$](OTs)$_2$, $C_{66}H_{62}O_6P_4PdS_2$ (1245.64) • 2 CH_2Cl_2 • C_6H_{14}: calcd. C

59.19, H 5.37, S 4.05; found C 59.26, H 5.25, S 3.94. ESI Mass Spectroscopy, m/z found (calcd): $[M - OTs]^+$ = 1072.73 (1073.19).

[Pd(oMeO-L2)(OAc)$_2$] (M(oMeO-L2)A) was prepared following method A. The product was obtained as a yellow powder, with an isolated yield of 81% (445 mg). Single crystals suitable for X-ray crystallography were obtained by layering a solution of the complex in dichloromethane with *n*-hexane. ^{1}H NMR (300 MHz, $CDCl_3$): δ 8.04 (q, 4H, *o*-Ph-*H*), 7.50 (t, 4H, *p*-Ph-*H*), 7.04 (t, 4H, OC=C-*H*), 6.92 (q, 4H, *m*-Ph-*H*), 3.72 (s, 12H, OCH_3), 2.63 (d, 4H, PCH_2), 1.36 (s, 6H, OC(O)CH_3) ppm; ^{31}P NMR (300 MHz, $CDCl_3$): δ 60.91 ppm. Elemental analyses for [Pd(oMeO-L2)(OAc)$_2$], $C_{34}H_{38}O_8P_2Pd$ (743.03) • 0.3 H_2O: calcd. C 54.52, H 5.20; found C 54.99, H 5.65. ESI Mass Spectroscopy, m/z found (calcd): $[M - OAc]^+$ = 682.75 (683.98).

[Pd(oMeO-L2)(OTs)$_2$] (M(oMeO-L2)T) was prepared following method B. The product was obtained as a yellow powder, with an isolated yield of 68% (487 mg). The compound was recrystallized by layering a solution of the complex in dichloromethane with diethyl ether. ^{1}H NMR (300 MHz, $OC(CH_3)_2$): δ 7.65 (m, 4H, *p*-Ph-*H* + *o*-Ph-*H*), 7.50 (d, 4H, *o*-OTs-*H*), 7.24 (t, 4H, OC=C-*H*), 7.09 (m, 8H, *m*-Ph-*H* + *m*-OTs-*H*), 3.80 (s, 12H, OCH_3), 3.05 (m, 4H, PCH_2), 2.29 (s, 6H, *p*-OTs-CH_3) ppm; ^{31}P NMR (300 MHz, $OC(CH_3)_2$): δ 57.50 ppm. Elemental analyses for [Pd(oMeO-L2)(OTs)$_2$], $C_{44}H_{46}O_{10}P_2PdS_2$ (967.33) • 1 CH_2Cl_2 • 0.25 $O(C_2H_3)_2$: calcd. C 51.60, H 4.75, S 2.97; found C 51.67, H 4.64, S 2.82. ESI Mass Spectroscopy, m/z found (calcd): $[M - OTs]^+$ = 794.77 (796.13).

[Pd(oMeO-L2)$_2$](OAc)$_2$ (B(oMeO-L2)A) was prepared following method C. The product was obtained as a yellow powder, with an isolated yield of 73% (460 mg). The compound was recrystallized by layering a solution of the complex in dichloromethane with diethyl ether. ^{1}H NMR (300 MHz, $CDCl_3$): δ 8.14 (br, 4H, *o*-Ph-*H*(ax)), 7.80 (t, 4H, *p*-Ph-*H*(ax)), 7.54 (m, 4H, *m*-Ph-*H*(ax)), 7.35 (m, 4H, *m*-Ph-*H*(eq)), 7.11 (d, 4H, OC=C-*H*(ax)), 6.88 (d, 4H, OC=C-*H*(eq)), 6.46 (t, 4H, *p*-Ph-*H*(eq)), 5.88 (br, 4H, *o*-Ph-*H*(eq)), 3.68 (s, 12H, OCH_3(ax)), 3.59 (s, 12H, OCH_3(eq)), 3.20 (m, 8H, PCH_2), 2.02 (s, 6H, OC(O)CH_3) ppm; ^{31}P NMR (300 MHz, $CDCl_3$): δ 55.83 ppm. Elemental analyses for [Pd(oMeO-L2)$_2$](OAc)$_2$, $C_{64}H_{70}O_{12}P_4Pd$ (1261.55) • 1 $O(C_2H_3)_2$ • 3 H_2O: calcd. C 52.63, H 5.70; found C 52.35, H 5.93. ESI Mass Spectroscopy, m/z found (calcd): $[M - 2\ OAc]^{2+}$ = 571.72 (571.73).

[Pd(oMeO-L2)$_2$](OTs)$_2$ (B(oMeO-L2)T) was prepared following method D. The product was obtained as a yellow powder, with an isolated yield of 30% (223 mg). The compound was recrystallized by layering a solution of the complex in dichloromethane with diethyl ether. ^{1}H NMR (300 MHz, $CDCl_3$): δ 8.08 (br, 4H, *o*-Ph-*H*(ax)), 7.89 (d, 4H, *o*-OTs-*H*), 7.81 (t, 4H, *p*-Ph-*H*(ax)), 7.50 (t, 4H, *m*-Ph-*H*(ax)), 7.26 (t, 4H, *m*-Ph-*H*(eq)), 7.12 (d, 4H, *m*-OTs-*H*), 6.97 (d, 4H, OC=C-*H*(ax)), 6.82 (d, 4H, OC=C-*H*(eq)), 6.56 (t, 4H, *p*-Ph-*H*(eq)), 5.84 (br, 4H, *o*-Ph-*H*(eq)), 3.67 (s, 12H, OCH_3(ax)), 3.52 (s, 12H, OCH_3(eq)), 3.03 (m, 8H, PCH_2), 2.33 (s, 6H, *p*-OTs-CH_3) ppm; ^{31}P NMR (300 MHz, $CDCl_3$): δ 55.95 ppm. Elemental analyses for [Pd(oMeO-L2)$_2$](OTs)$_2$, $C_{74}H_{78}O_{14}P_4PdS_2$ (1485.85) • 2 CH_2Cl_2 • 2 $O(C_2H_3)_2$: calcd. C 55.93, H 5.70, S 3.63; found C 56.04, H 5.88, S 3.80. ESI Mass Spectroscopy, m/z found (calcd): $[M - OTs]^+$ = 1072.73 (1073.19).

[Pd(L3)(OAc)$_2$] (M(L3)A) was prepared following method A. The product was obtained as a yellow powder, with an isolated yield of 93% (438 mg). The compound was recrystallized by layering a solution of the complex in dichloromethane with diethyl ether. ^{1}H NMR (300 MHz, $CHCl_3$): δ 7.72 (m, 8H, *m*-Ph-*H*), 7.34 (m, 12H, *o*-Ph-*H* + *p*-Ph-*H*), 2.51 (m, 4H, PCH_2), 2.15 (m, 2H, PCH_2CH_2), 1.34 (s, 6H, OC(O)CH_3) ppm; ^{31}P NMR (300 MHz, $CHCl_3$): δ 9.74 ppm. Elemental analyses for [Pd(L3)(OAc)$_2$], $C_{31}H_{32}O_4P_2Pd$ (636.95) • 0.5 CH_2Cl_2 • 0.5 $O(C_2H_3)_2$: calcd. C 56.16, H 5.35; found C 56.64, H 5.33. ESI Mass Spectroscopy, m/z found (calcd): $[M - OAc]^+$ = 576.65 (577.91).

[Pd(L3)(OTs)$_2$] (M(L3)T) was prepared following method B. The product was obtained as a yellow powder, with an isolated yield of 78% (497 mg). The compound was recrystallized by layering a solution of the complex in dichloromethane with diethyl ether. ^{1}H NMR (300 MHz, $CHCl_3$): δ 7.67 (q, 8H, *o*-Ph-*H*), 7.41 (m, 8H, *p*-Ph-*H* + *o*-OTs-*H*), 7.26 (t, 8H, *m*-Ph-*H*), 6.86 (d, 4H, *m*-OTs-*H*), 2.83 (m, 4H, PCH_2), 2.25 (m, 2H, PCH$_2$CH_2), 2.31 (s, 6H, *p*-OTs-CH_3) ppm; ^{31}P NMR (300 MHz, $CHCl_3$): δ 15.88 ppm. Elemental analyses for [Pd(L3)(OTs)$_2$], $C_{41}H_{40}O_6P_2PdS_2$ (861.25) • 1.3 H_2O: calcd. C 55.63, H 4.86, S 5.15; found C 55.73, H 4.79, S 5.51. ESI Mass Spectroscopy, m/z found (calcd): $[M - OTs]^+$ = 688.71 (689.07).

[Pd(L3X)(OAc)$_2$] (M(L3X)A) was prepared following method A. The product was obtained as a yellow powder, with an isolated yield of 96% (472 mg). The compound was recrystallized by layering a solution of the complex in dichloromethane with diethyl ether. ^{1}H NMR (300 MHz, $CHCl_3$): δ 7.90 (m, 8H, *o*-Ph-*H*), 7.44 (m, 12H, *m*-Ph-*H* + *p*-Ph-*H*), 2.29 (d, 4H, PCH_2), 0.91 (s, 6H, CCH_3), 1.44 (s, 6H, OC(O)CH_3) ppm; ^{31}P NMR (300 MHz, $CHCl_3$): δ 16.35 ppm. Elemental analyses for [Pd(L3X)(OAc)$_2$], $C_{33}H_{36}O_4P_2Pd$ (665.00) • 0.25 CH_2Cl_2 • 0.5 O(C_2H_3)$_2$: calcd. C 58.62, H 5.65; found C 58.66, H 5.57. ESI Mass Spectroscopy, m/z found (calcd): $[M - OAc]^+$ = 604.77 (605.10).

[Pd(L3X)(OTs)$_2$] (M(L3X)T) was prepared following method B. The product was obtained as a yellow powder, with an isolated yield of 83% (546 mg). The compound was recrystallized by layering a solution of the complex in dichloromethane with diethyl ether. ^{1}H NMR (300 MHz, CH_3OH): δ 7.88 (d, 4H, *o*-OTs-*H*), 7.58 (br, 8H, *o*-Ph-*H*), 7.29 (m, 16H, *m*-Ph-*H* + *p*-Ph-*H* + *m*-OTs-*H*), 2.59 (br, 4H, PCH_2), 2.38 (s, 6H, *p*-OTs-CH_3), 0.26 (s, 6H, CCH_3) ppm; ^{31}P NMR (300 MHz, CH_3OH): δ 6.72 ppm. Elemental analyses for [Pd(L3X)(OTs)$_2$], $C_{43}H_{44}O_6P_2PdS_2$ (889.30) • CH_2Cl_2 • 1.25 O(C_2H_5)$_2$: calcd. C 55.29, H 5.30, S 4.52; found C 55.37, H 5.19, S 4.69. ESI Mass Spectroscopy, m/z found (calcd): $[M - OTs]^+$ = 688.71 (689.07).

[Pd(L3X)$_2$](OTs)$_2$ (B(L3X)T) was prepared following method D. The product was obtained as a yellow powder, with an isolated yield of 92% (612 mg). The compound was recrystallized by layering a solution of the complex in dichloromethane with diethyl ether. ^{1}H NMR (300 MHz, CH_3OH): δ 8.00 (d, 4H, *o*-OTs-*H*), 7.60 (br, 16H, *o*-Ph-*H*), 7.26 (m, 28H, *m*-Ph-*H* + *p*-Ph-*H* + *m*-OTs-*H*), 2.62 (br, 8H, PCH_2), 2.38 (s, 6H, *p*-OTs-CH_3), 0.26 (s, 12H, CCH_3) ppm; ^{31}P NMR (300 MHz, CH_3OH): δ 5.63 ppm. Elemental analyses for [Pd(L3X)$_2$](OTs)$_2$, $C_{72}H_{74}O_6P_4PdS_2$ (1329.80) • 1.25 CH_2Cl_2 • O(C_2H_3)$_2$: calcd. C 63.83, H 6.00, S 4.33; found C 63.73, H 6.24, S 4.62. ESI Mass Spectroscopy, m/z found (calcd): $[M - OTs]^+$ = 1156.91 (1157.28).

[Pd(oMeO-L3)(OAc)$_2$] (M(oMeO-L3)A) was prepared following method A. The product was obtained as a yellow powder, with an isolated yield of 87% (487 mg). Single crystals suitable for X-ray crystallography were obtained by layering of *n*-hexane with a solution of the complex in dichloromethane. ^{1}H NMR (300 MHz, $CDCl_3$): δ 8.25 (br, 4H, *o*-Ph-*H*), 7.50 (t, 4H, *p*-Ph-*H*), 7.08 (br, 4H, *m*-Ph-*H*), 6.94 (d, 4H, OC=C-*H*), 3.76 (s, 12H, OCH_3), 2.44 (m, 4H, PCH_2), 1.95 (m, 2H, PCH$_2$CH_2), 1.26 (s, 6H, OC(O)CH_3) ppm; ^{31}P NMR (300 MHz, CDCl3): δ 14.50 ppm. Elemental analyses for [Pd(oMeO-L3)(OAc)$_2$], $C_{35}H_{40}O_8P_2Pd$ (757.05) • CH_2Cl_2: calcd. C 54.35, H 6.08; found C 54.18, H 6.21. ESI Mass Spectroscopy, m/z found (calcd): $[M - OAc]^+$ = 698.62 (698.01).

[Pd(oMeO-L3)$_2$](OAc)$_2$ (B(oMeO-L3)A) was prepared following method C. The product was obtained as a yellow powder, with an isolated yield of 94% (606 mg). The compound was recrystallized by layering a solution of the complex in dichloromethane with diethyl ether. ^{1}H NMR (300 MHz, CH_3OH): δ 8.59 (br, 4H, *o*-Ph-*H*(ax)), 7.74 (t, 4H, *m*-Ph-*H*(ax)), 7.46 (t, 4H, *p*-Ph-*H*(ax)), 7.30 (t, 4H, *p*-Ph-*H*(eq)), 7.05 (m, 8H, OC=C-*H*(ax + eq)), 6.61 (t, 4H, *m*-Ph-*H*(eq)), 5.91 (br, 4H, *o*-Ph-*H*(eq)), 4.23 (s, 12H, OCH_3(ax)), 3.42 (s, 12H, OCH_3(eq)), 2.90 (m, 4H, PCH_2(ax)), 2.38 (m, 4H, PCH_2(eq)), 1.95 (m, 2H, PCH$_2$CH_2), 1.87 (s, 6H, OC(O)CH_3) ppm; ^{31}P NMR (300 MHz, CH_3OH): δ 5.56 ppm. Elemental analyses for [Pd(oMeO-L3)$_2$](OAc)$_2$, $C_{66}H_{74}O_{12}P_4Pd$

(1289.60) • CH_2Cl_2: calcd. C 55.96, H 6.58; found C 55.91, H 6.58. ESI Mass Spectroscopy, m/z found (calcd): $[M - 2\ OAc]^{2+}$ = 584.83 (585.15).

[Pd(oMeO-L3)$_2$](OTs)$_2$ (B(oMeO-L3)T) was prepared following method D. The product was obtained as a yellow powder, with an isolated yield of 72% (545 mg). The compound was recrystallized by layering a solution of the complex in dichloromethane with diethyl ether. ^{1}H NMR (300 MHz, $CHCl_3$): δ 8.51 (br, 4H, *o*-Ph-*H*(ax)), 7.96 (d, 4H, *o*-OTs-*H*), 7.73 (t, 4H, *m*-Ph-*H*(ax)), 7.64 (t, 4H, *p*-Ph-*H*(ax)), 7.20 (m, 8H, *p*-Ph-*H*(eq) + *m*-OTs-*H*), 6.99 (d, 4H, OC=C-*H*(ax)), 6.83 (d, 4H, OC=C-*H*(eq)), 6.47 (t, 4H, *m*-Ph-*H*(eq)), 5.82 (br, 4H, *o*-Ph-*H*(eq)), 4.33 (s, 12H, OCH_3(ax)), 3.38 (s, 12H, OCH_3(eq)), 2.85 (m, 4H, PCH_2(ax)), 2.36 (s, 6H, *p*-OTs-CH_3), 2.25 (m, 4H, PCH_2(eq)), 1.52 (br, 4H, PCH$_2$CH_2) ppm; ^{31}P NMR (300 MHz, $CHCl_3$): δ 4.81 ppm. Elemental analyses for [Pd(oMeO-L3)$_2$](OTs)$_2$, $C_{76}H_{82}O_{14}P_4PdS_2$ (1513.90) • 0.25 CH_2Cl_2 • 0.25 O(C_2H_3)$_2$: calcd. C 59.72, H 5.52, S 3.96; found C 59.48, H 5.87, S 3.96. ESI Mass Spectroscopy, m/z found (calcd): $[M - OTs]^+$ = 1340.53 (1341.30).

[Pd(oMeO-L3X)(OAc)$_2$] (M(oMeO-L3X)A) was prepared following method A. The product was obtained as a yellow powder, with an isolated yield of 96% (558 mg). Single crystals suitable for X-ray crystallography were obtained by layering of *n*-hexane with a solution of the complex in dichloromethane. ^{1}H NMR (300 MHz, $CDCl_3$): δ 8.15 (br, 4H, *o*-Ph-*H*), 7.51 (t, 4H, *m*-Ph-*H*), 7.07 (m, 4H, *p*-Ph-*H*), 6.92 (d, 4H, OC=C-*H*), 3.86 (s, 12H, OCH_3), 2.58 (d, 4H, PCH_2), 1.20 (s, 6H, OC(O)CH_3), 0.33 (s, 6H, CCH_3) ppm; ^{31}P NMR (300 MHz, CDCl3): δ 20.84 ppm. Elemental analyses for [Pd(oMeO-L3X)(OAc)$_2$], $C_{37}H_{44}O_8P_2Pd$ (785.11) • CH_2Cl_2 • 0.7 C_6H_{12}: calcd. C 54.51, H 6.01; found C 54.39, H 5.96. ESI Mass Spectroscopy, m/z found (calcd): $[M - OAc]^+$ = 724.77 (726.06).

[Pd(oMeO-L3X)$_2$](OAc)$_2$ (B(oMeO-L3X)A) was prepared following method C. The product was obtained as a yellow powder, with an isolated yield of 97% (653 mg). The compound was recrystallized by layering a solution of the complex in dichloromethane with diethyl ether. ^{1}H NMR (300 MHz, CH_3OH): δ 8.36 (br, 4H, *o*-Ph-*H*(ax)), 7.64 (t, 4H, *m*-Ph-*H*(ax)), 7.30 (m, 8H, *p*-Ph-*H*(ax) + *p*-Ph-*H*(eq)), 7.11 (d, 4H, OC=C-*H*(ax)), 6.92 (d, 4H, OC=C-*H*(eq)), 6.70 (t, 4H, *m*-Ph-*H*(eq)), 6.48 (br, 4H, *o*-Ph-*H*(eq)), 4.26 (s, 12H, OCH_3(ax)), 3.41 (s, 12H, OCH_3(eq)), 2.78 (d, 4H, PCH_2(ax)), 2.44 (d, 4H, PCH_2(eq)), 1.88 (s, 6H, OC(O)CH_3), 0.22 (s, 12H, CCH_3) ppm; ^{31}P NMR (300 MHz, CH_3OH): δ 10.88 ppm. Elemental analyses for [Pd(oMeO-L3X)$_2$](OAc)$_2$, $C_{70}H_{82}O_{12}P_4Pd$ (1345.71) • 2.5 CH_2Cl_2 • 2.5 O(C_2H_3)$_2$: calcd. C 57.28, H 6.44; found C 56.97, H 6.90. ESI Mass Spectroscopy, m/z found (calcd): $[M - 2\ OAc]^{2+}$ = 613.43 (613.18).

[Pd(oMeO-L3X)$_2$](OTs)$_2$ (B(oMeO-L3X)T) was prepared following method D. The product was obtained as a yellow powder, with an isolated yield of 89% (699 mg). Single crystals suitable for X-ray crystallography were obtained by layering of hexane with a solution of the complex in acetone. ^{1}H NMR (300 MHz, $CDCl_3$): δ 8.29 (br, 4H, *o*-Ph-*H*(ax)), 7.95 (d, 4H, *o*-OTs-*H*), 7.56 (m, 8H, *p*-Ph-*H*(ax) + *m*-Ph-*H*(ax)), 7.16 (m, 8H, *p*-Ph-*H*(eq) + *m*-OTs-*H*), 7.07 (d, 4H, OC=C-*H*(ax)), 6.68 (d, 4H, OC=C-*H*(eq)), 6.53 (t, 4H, *m*-Ph-*H*(eq)), 6.34 (br, 4H, *o*-Ph-*H*(eq)), 4.38 (s, 12H, OCH_3(ax)), 3.38 (s, 12H, OCH_3(eq)), 2.70 (d, 4H, PCH_2(ax)), 2.36 (s, 6H, *p*-OTs-CH_3), 2.30 (d, 4H, PCH_2(eq)), 0.12 (s, 12H, CCH_3) ppm; ^{31}P NMR (300 MHz, $CDCl_3$): δ 10.10 ppm. Elemental analyses for [Pd(oMeO-L3X)$_2$](OTs)$_2$, $C_{80}H_{90}O_{14}P_4PdS_2$ (1570.01) • 0.25 CH_2Cl_2 • 0.5 C_6H_{14}: calcd. C 58.87, H 5.79, S 3.92; found C 58.40, H 5.99, S 3.51. ESI Mass Spectroscopy, m/z found (calcd): $[M - OTs]^+$ = 1396.47 (1396.37).

[Pd(oMeO-L3X^R)(OAc)$_2$] (M(oMeO-L3X^R)A) was prepared following method A. The product was obtained as a yellow powder, with an isolated yield of 94% (624 mg). Single crystals suitable for X-ray crystallography were obtained by layering of *n*-hexane with a solution of the complex in acetone. ^{1}H NMR (300 MHz, $CDCl_3$): δ 8.50 (br, 4H, *o*-Ph-*H*), 7.52 (br, 4H, *m*-Ph-*H*), 7.08 (br, 4H, *p*-Ph-*H*), 6.94 (d, 4H, OC=C-*H*), 3.88 (s, 12H, OCH_3), 3.09 (s, 4H, CCH_2O), 2.68 (s, 4H, PCH_2),

1.57 (m, 4H, OCCH_2), 1.37 (m, 6H, OCCH$_2$CH_2 + OCCH$_2$CH$_2$CH_2), 1.21 (s, 6H, OC(O)CH_3) ppm; ^{31}P NMR (300 MHz, $CDCl_3$): δ 18.05 ppm. Elemental analyses for [Pd(oMeO-L3X^R)(OAc)$_2$], $C_{43}H_{52}O_{10}P_2Pd$ (897.23): calcd. C 57.56, H 5.84; found C 57.00, H 6.16. ESI Mass Spectroscopy, m/z found (calcd): [M –OAc]$^+$ = 836.82 (838.19).

[Pd(oMeO-L3X^R)$_2$](OAc)$_2$ (B(oMeO-L3X^R)A) was prepared following method C. The product was obtained as a yellow powder, with an isolated yield of 70% (550 mg). The compound was recrystallized by layering a solution of the complex in dichloromethane with *n*-hexane. ^{1}H NMR (300 MHz, CH_3OH): δ 8.35 (br, 4H, *o*-Ph-*H*(ax)), 7.34 (t, 4H, *p*-Ph-*H*(ax)), 7.29 (t, 4H, *p*-Ph-*H*(eq)), 7.14 (d, 4H, OC=C-*H*(ax)), 6.97 (d, 4H, OC=C-*H*(eq)), 6.78 (t, 4H, *m*-Ph-*H*(ax)), 6.72 (t, 4H, *m*-Ph-*H*(eq)), 6.48 (br, 4H, *o*-Ph-*H*(eq)), 4.30 (s, 12H, OCH_3(ax)), 3.42 (s, 12H, OCH_3(eq)), 2.88 (d, 4H, PCH_2(ax)), 2.56 (m, 12H, PCH_2(eq) + CCH_2O), 1.88 (s, 6H, OC(O)CH_3), 1.37 (m, 8H, OCCH_2), 1.23 (m, 12H, OCCH$_2$CH_2 + OCCH$_2$CH$_2$C*H*2) ppm; ^{31}P NMR (300 MHz, CH_3OH): δ 8.82 ppm. Elemental analyses for [Pd(oMeO-L3X^R)$_2$](OAc)$_2$, $C_{82}H_{98}O_{16}P_4Pd$ (1569.96) • 0.5 CH_2Cl_2 • 0.5 C_6H_{14}: calcd. C 62.03, H 6.45; found C 62.00, H 6.46. ESI Mass Spectroscopy, m/z found (calcd): [M – 2 OAc]$^{2+}$ = 725.15 (725.23).

[Pd(oMeO-L3X^R)$_2$](OTs)$_2$ (B(oMeO-L3X^R)T) was prepared following method D. The product was obtained as a yellow powder, with an isolated yield of 63% (565 mg). The compound was recrystallized by layering a solution of the complex in dichloromethane with *n*-hexane. ^{1}H NMR (300 MHz, $CHCl_3$): δ 8.28 (br, 4H, *o*-Ph-*H*(ax)), 8.00 (d, 4H, *o*-OTs-*H*), 7.60 (m, 8H, *p*-Ph-*H*(ax) + *m*-Ph-*H*(ax)), 7.17 (m, 20H, OC=C-*H*(ax) + *p*-Ph-*H*(eq) + *m*-OTs-*H*), 6.74 (d, 4H, OC=C-*H*(eq)), 6.54 (t, 4H, *m*-Ph-*H*(eq)), 6.34 (br, 4H, *o*-Ph-*H*(eq)), 4.44 (s, 12H, OCH_3(ax)), 3.40 (s, 12H, OCH_3(eq)), 2.73 (d, 4H, PCH_2(ax)), 2.44 (m, 18H, PCH_2(eq) + CCH_2O + *p*-OTs-CH_3), 1.42 (br, 8H, OCCH_2), 1.23 (br, 12H, OCCH$_2$CH_2 + OCCH$_2$CH$_2$CH_2) ppm; ^{31}P NMR (300 MHz, $CHCl_3$): δ 8.03 ppm. Elemental analyses for [Pd(oMeO-L3X^R)$_2$](OTs)$_2$, $C_{92}H_{106}O_{18}P_4PdS_2$ (1794.26) • 0.33 CH_2Cl_2: calcd. C 60.84, H 5.90, S 3.50; found C 60.84, H 5.90, S 3.02. ESI Mass Spectroscopy, m/z found (calcd): [M – 2 OTs]$^{2+}$ = 726.50 (725.94).

[Pd(L4)(OAc)$_2$] (M(L4)A) was prepared following method A. The product was obtained as a yellow powder, with an isolated yield of 96% (463 mg). The compound was recrystallized by layering a solution of the complex in dichloromethane with diethyl ether. ^{1}H NMR (300 MHz, CH_3OH): δ 7.63 (q, 8H, *o*-Ph-*H*), 7.47 (t, 4H, *p*-Ph-*H*), 7.34 (t, 8H, *m*-Ph-*H*), 2.44 (br, 4H, PCH_2), 1.93 (m, 4H, PCH$_2$CH_2), 1.32 (s, 6H, OC(O)CH_3) ppm; ^{31}P NMR (300 MHz, CH_3OH): δ 28.56 ppm. Elemental analyses for [Pd(L4)(OAc)$_2$], $C_{32}H_{34}O_4P_2Pd$ (650.98) • 1.5 CH_2Cl_2: calcd. C 51.69, H 4.79; found C 51.88, H 4.93. ESI Mass Spectroscopy, m/z found (calcd): [M – OAc]$^+$ = 590.73 (591.08).

[Pd(L4)(OTs)$_2$] (M(L4)T) was prepared following method B. The product was obtained as a yellow powder, with an isolated yield of 92% (596 mg). The compound was recrystallized by layering a solution of the complex in dichloromethane with diethyl ether. ^{1}H NMR (300 MHz, $CHCl_3$): δ 7.70 (t, 8H, *p*-Ph-*H*), 7.54 (t, 8H, *m*-Ph-*H*), 7.40 (m, 8H, *o*-Ph-*H* + *o*-OTs-*H*), 6.93 (d, 4H, *m*-OTs-*H*), 2.58 (br, 4H, PCH_2), 2.31 (s, 6H, *p*-OTs-CH_3), 2.15 (m, 4H, PCH$_2$CH_2) ppm; ^{31}P NMR (300 MHz, $CHCl_3$): δ 32.80 ppm. Elemental analyses for [Pd(L4)(OTs)$_2$], $C_{42}H_{42}O_6P_2PdS_2$ (875.28) • 1.25 CH_2Cl_2 • 1.25 O(C_2H_3)$_2$: calcd. C 54.08, H 5.13, S 5.02; found C 54.22, H 5.00, S 5.13. ESI Mass Spectroscopy, m/z found (calcd): [M – OTs]$^+$ = 702.62 (703.08).

References

[1] E. Drent, P. H. M. Budzelaar, *Chem. Rev.* **1996**, *96*, 663.
[2] C. Bianchini, A. Meli, *Coord. Chem. Rev.* **2002**, *225*, 35.
[3] F. Paul, *Coord. Chem. Rev.* **2000**, *203*, 269.
[4] E. Drent, P. W. N. M. van Leeuwen, EU 0086281A1, **1982**.
[5] E. Drent, EU 0231045A2, **1987**.
[6] F. Ragaini, C. Cognolato, M. Gasperini, S. Cenini, *Angew. Chem.* **2003**, *42*, 2886.
[7] E. Drent, *Pure Appl. Chem.* **1990**, *62*, 661.
[8] P. Wehman, L. Borst, P. C. J. Kamer, P. W. N. M. van Leeuwen, *J. Mol. Catal. A-Chem.* **1996**, *112*, 23.
[9] A. Marson, A. B. van Oort, W. P. Mul, *Eur. J. Inorg. Chem.* **2002**, 3028.
[10] E. Drent, EU 224292, **1987**.
[11] A. Bontempi, E. Alessio, G. Chanos, G. Mestroni, *J. Mol. Catal.* **1987**, *42*, 67.
[12] S. Cenini, F. Ragaini, M. Pizzotti, F. Porta, G. Mestroni, E. Alessio, *J. Mol. Catal.* **1991**, *64*, 179.
[13] R. Santi, A. M. Romano, F. Panella, G. Mestroni, A. Sessanti, A. S. o Santi, *J. Mol. Catal. A-Chem.* **1999**, *144*, 41.
[14] P. Leconte, F. Metz, A. Mortreux, J. A. Osborn, F. Paul, F. Petit, A. Pillot, *J. Chem. Soc.-Chem. Commun.* **1990**, 1616.
[15] P. Wehman, V. E. Kaasjager, W. G. J. de Lange, F. Hartl, P. C. J. Kamer, P. W. N. M. van Leeuwen, J. Fraanje, K. Goubitz, *Organometallics* **1995**, *14*, 3751.
[16] P. Wehman, G. C. Dol, E. R. Moorman, P. C. J. Kamer, P. W. N. M. van Leeuwen, J. Fraanje, K. Goubitz, *Organometallics* **1994**, *13*, 4856.
[17] P. Wehman, PhD thesis, University of Amsterdam (UvA) **1995**.
[18] F. Ragaini, M. Gasperini, S. Cenini, *Adv. Synth. Catal.* **2004**, *346*, 63.
[19] F. Ragaini, *Dalton Trans.* **2009**, 6251.
[20] J. H. Grate, D. R. Hamm, D. H. Valentine, US 4.603.216, **1986**.
[21] P. Wehman, R. E. Rulke, V. E. Kaasjager, P. C. J. Kamer, H. Kooijman, A. L. Spek, C. J. Elsevier, K. Vrieze, P. W. N. M. van Leeuwen, *J. Chem. Soc.-Chem. Commun.* **1995**, 331.
[22] D. Cremer, J. A. Pople, *J. Am. Chem. Soc.* **1975**, *97*, 1354.
[23] C. Bianchini, A. Meli, W. Oberhauser, *Dalton Trans.* **2003**, 2627.
[24] A. Marson, A. B. van Oort, W. P. Mul, *Eur. J. Inorg. Chem.* **2002**, *11*, 3028.
[25] F. A. Cotton, S. Han, *Rev. De Chim. Min.* **1983**, *20*, 496.
[26] A. G. Orpen, L. Brammer, F. H. Allen, O. Kennard, D. G. Watson, R. Taylor, *J. Chem. Soc. Dalton Trans.* **1989**, S1.
[27] I. M. Angulo, E. Bouwman, M. Lutz, W. P. Mul, A. L. Spek, *Inorg. Chem.* **2001**, *40*, 2073.
[28] C. Bianchini, A. Meli, W. Oberhauser, A. M. Segarra, C. Claver, E. J. G. Suarez, *J. Mol. Catal. A-Chem.* **2007**, *265*, 292.
[29] M. Brookhart, M. L. H. Green, G. Parkin, *Proc. Natl. Acad. Sci. U. S. A.* **2007**, *104*, 6908.
[30] J. F. Malone, C. M. Murray, M. H. Charlton, R. Docherty, A. J. Lavery, *J. Chem. Soc, Faraday Trans.* **1997**, *93*, 3429.
[31] C. Bianchini, H. M. Lee, A. Meli, W. Oberhauser, M. Peruzzini, F. Vizza, *Organometallics* **2002**, *21*, 16.
[32] C. Bianchini, P. Bruggeller, C. Claver, G. Czermak, A. Dumfort, A. Meli, W. Oberhauser, E. J. G. Suarez, *Dalton Trans.* **2006**, 2964.
[33] I. M. Angulo, E. Bouwman, R. van Gorkum, S. M. Lok, M. Lutz, A. L. Spek, *J. Mol. Catal. A-Chem.* **2003**, *202*, 97.
[34] M. E. Jung, *J. Am. Chem. Soc.* **1991**, *113*, 224.
[35] P. V. R. Schleyer, *J. Am. Chem. Soc.* **1961**, *83*, 1368.
[36] T. Hayashi, M. Konishi, Y. Kobori, M. Kumada, T. Higuchi, K. Hirotsu, *J. Am. Chem. Soc.* **1984**, *106*, 158.

[37] R. J. van Haaren, K. Goubitz, J. Fraanje, G. P. F. van Strijkdonk, H. Oevering, B. Coussens, J. N. H. Reek, P. C. J. Kamer, P. W. N. M. van Leeuwen, *Inorg. Chem.* **2001**, *40*, 3363.
[38] A. G. Avent, R. B. Bedford, P. A. Chaloner, S. Z. Dewa, P. B. Hitckcock, *J. Chem. Soc., Dalton Trans.* **1996**, 4633.
[39] L. Brandsma, H. D. Verkruijsse, *Synth. Commun.* **1990**, *20*, 2273.
[40] P. H. M. Budzelaar, J. A. van Doorn, N. Meijboom, *Recl. Trav. Chim. Pays-Bas-J. Roy. Neth. Chem. Soc.* **1991**, *110*, 420.
[41] J. A. van Doorn, PhD thesis, University of Amsterdam (UvA) **1991**.
[42] W. Hewertson, H. R. Watson, *J. Chem. Soc.* **1962**, 1490.
[43] F. Bickelhaupt, US 4874897, **1989**.
[44] W. Eilenberg, EU 364046, **1991**.
[45] J. A. van Doorn, US 4994592, **1991**.
[46] R. van Ginkel, US 6548708, **2003**.
[47] E. Drent, US 5091587, **1992**.
[48] C. F. Hobbs, US 4120901, **1987**.
[49] P. W. Clark, B. J. Mulraney, *J. Organomet. Chem.* **1981**, *217*, 51.
[50] J. M. Brown, B. A. Murrer, *Tetrahedron Lett.* **1980**, *21*, 581.
[51] R. L. Wife, A. B. van Oort, J. A. van Doorn, P. W. N. M. van Leeuwen, *Synthesis* **1983**, *1*, 71.
[52] Z. Otwinowski, W. Minor, *Methods in Enzymology, Vol. 276*, Academic press, **1997**.
[53] A. J. M. Duisenberg, L. M. J. Kroon-Batenburg, A. M. M. Schreurs, **2003**, *36*, 220.
[54] A. Altomare, M. C. Burla, M. Camalli, G. L. Cascarano, C. Giacovazzo, A. Guagliardi, A. G. G. Moliterni, G. Polidori, R. Spagna, *J. Appl. Cryst.* **1999**, *32*, 115.
[55] G. M. Sheldrick, *Acta Cryst.* **2008**, *A64*, 112.
[56] P. T. A. Beurskens, G.; Beurskens, G.; Bosman, W. P.; Garcia-Granda, S.; Gould, R. O.; Smith, J. M. M.; Smykalla, C., *The DIRDIF97 program system: Technical report of the Crystallography Laboratory; University of Nijmegen, The Netherlands* **1997**
[57] A. L. Spek, *J. Appl. Cryst.* **2003**, *36*, 7.